

# A compact low-noise passively mode-locked Er-doped femtosecond all-fiber laser with 2.68 GHz fundamental repetition rate

Jiazheng Song,<sup>1,2</sup> Hushan Wang,<sup>1,2</sup> Xinning Huang,<sup>1,2</sup> XiaoHong Hu,<sup>1</sup> Ting Zhang,<sup>1,2</sup> Yishan Wang,<sup>1</sup> Yuanshan Liu,<sup>1\*</sup> and Jianguo Zhang<sup>1,3,4</sup>

<sup>1</sup> State Key Laboratory of Transient Optics and Photonics, Xi'an Institute of Optics and Precision Mechanics, Chinese Academy of Sciences, Xi'an 710119, China

<sup>2</sup> University of Chinese Academy of Sciences, Beijing 100049, China

<sup>3</sup> Department of Engineering and Design, London South Bank University, 103 Borough Road, London SE1 0AA, UK

<sup>4</sup> zhangja@lsbu.ac.uk

\* liuyuanshan@opt.ac.cn,

**Abstract:** A passively mode-locked Er-doped fiber laser with a fundamental repetition rate of 2.68 GHz is reported. The oscillator operating at a central wavelength of 1558.35 nm has a compact, robust structure and low-noise performance. The timing jitter integrated from 30 MHz down to 300 Hz is 82.5 fs and the timing jitter performance is analyzed based on the theory model. The amplification and compression of the high repetition rate optical pulses are also investigated. After a three-stage amplifier, the average power is boosted to 430 mW. Meanwhile, based on the nonlinear self-phase modulation effect, the spectral bandwidth is broadened from 7.56 nm to 19.2 nm and the corresponding pulse width is compressed to 244 fs.

© 2018 Optical Society of America

## 1. Introduction

High-repetition-rate (over 1 GHz) femtosecond lasers play an important role in many applications, including optical arbitrary waveform generation [1, 2], high precision frequency metrology [3, 4], ultrastable microwave signal generation [5-7], high speed optical sampling [8-10], and high resolution astronomical spectrographs (astro-combs) [11-14]. Over the past decade multi-gigahertz repetition rate ultrafast lasers have been experimentally developed [15-27]. Chen et al. demonstrated a 3 GHz mode-locked femtosecond laser by using a 1cm highly Yb-doped phosphate glass fiber [15]. The integrated relative intensity noise (RIN) between 10 Hz and 10 MHz is 0.14%. Recently a 5 GHz Yb-doped fiber laser was reported [16]. This is the highest fundamental pulse repetition rate ever reported at 1  $\mu$ m wavelength region. However, in both of their works the phase noise is not measured. For Tm-doped fiber lasers (TDFLs), a gigahertz passively mode-locked TDFL is proposed and demonstrated by Cheng et al. by using a homemade highly Tm-doped barium gallo-germanate glass fiber [19]. The timing jitter integrated from 10 MHz down to 10 Hz in the TDFL is measured as 1.705 ps. At wavelength around 1.55  $\mu$ m, Martinez et al. reported a 19.45 GHz Er:Yb-doped fiber laser mode locked by a carbon nanotube based saturable absorber (CNT-SA), which is the highest fundamental repetition rate among the reported fiber lasers to date [21], the timing jitter in this paper is investigated following the method described in [28], and the result is 372 fs for the laser operating at 4.24 GHz. A stable, efficient, low timing jitter fiber laser with a repetition rate of 1 GHz is demonstrated by Byun et al. [24], which is monolithic and thermal-damage-free by inserting an undoped fiber piece between the Er-doped fiber (EDF) and the butt-coupled saturable Bragg reflector (SBR). The single sideband phase noise is

measured at 967.3 MHz and the timing jitter integrated from 10 MHz down to 1 kHz is 22 fs. A 12 GHz Er:Yb-doped picosecond fiber laser is developed by using polarization-maintaining fibers and a semiconductor saturable-absorber mirror (SESAM) with high modulation depth [26]. In contrast to other mode-lockers (e.g., CNT-SA, nonlinear polarization evolution and nonlinear optical loop mirror), the passively mode-locked fiber laser using a SESAM as mode-locker is more reliable due to the high threshold of thermal damage and compact, stable structure. It is also noteworthy that high pulse energy and short pulse duration are required in many applications such as optical frequency comb, low noise microwave signal generation and so on. So far most works on high repetition rate femtosecond fiber lasers focus on how to generate high repetition rate pulses, it is important to make investigations on the amplification and compression of the optical pulses.

In this paper, we experimentally develop a passively mode-locked oscillator with a fundamental pulse repetition rate of 2.68 GHz. The amplification and compression of the output pulses after the oscillator are also investigated. The compact and robust oscillator delivers mode-locked pulses with a central wavelength of 1558.35 nm and spectral bandwidth of 7.56 nm. The single sideband phase noise is measured at 2.68 GHz and a low timing jitter of 82.5 fs integrated from 30 MHz down to 300 Hz is obtained. Detailed analysis on the time jitter is made and the approach to optimizing the timing jitter is also proposed. After a three-stage amplification and compression, a broadened optical spectrum with a bandwidth of 19.2 nm, a compressed pulse duration of 244 fs and an average optical power of 430 mW are achieved.

## 2. Experimental Setup

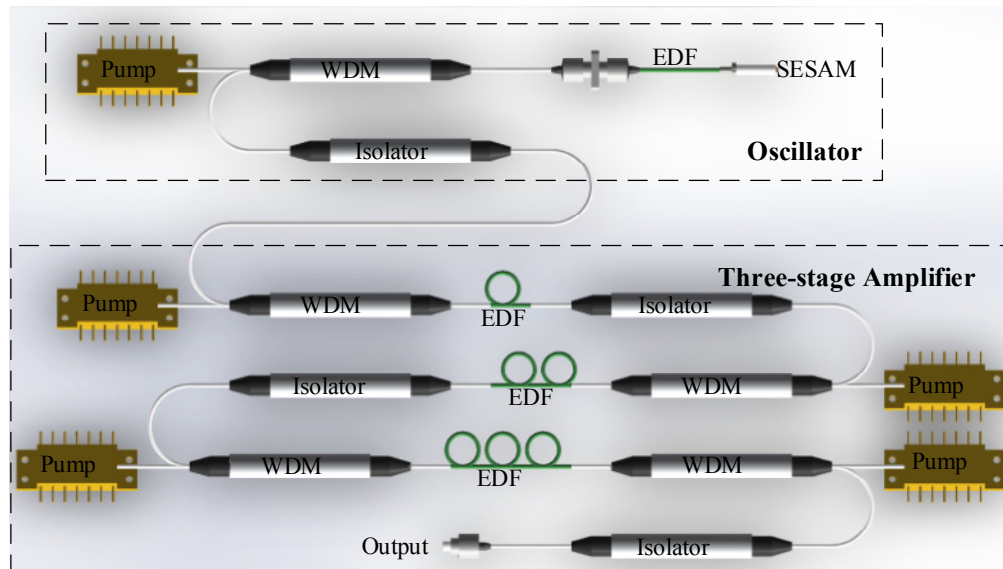


Fig. 1. Schematic experimental setup of the 2.68 GHz oscillator and the three-stage amplifier

Figure 1 illustrates the schematic of the experimental setup which consists of a 2.68 GHz EDF oscillator and a three-stage EDF amplifier. A 3.8 cm commercial EDF (Liekki Er110-4/125) with a dispersion parameter of  $13.3 \text{ fs}^2/\text{mm}$  is used in the oscillator as the gain medium. The gain fiber is secured with epoxy in 127  $\mu\text{m}$  inner diameter ceramic ferrules, both ends of which are flat polished. A coated fiber ferrule, as the output coupler, is connected to one end of the polished gain fiber in a mating sleeve. The output coupler shows a high reflectivity of 99.8% at 1550 nm as well as a high transmittance of over 98% at 976 nm to reduce the pump loss. The other end of the gain fiber is butt-coupled to a SESAM which is used as the

mode-locker, such a structure could promise the spot area of the light injecting on the surface of the SESAM is small enough for the oscillator to get self-start even under the condition of low intracavity optical pulse energy. The anomalous dispersion of the SESAM (produced by Batop GmbH) is  $\sim 455 \text{ fs}^2$  at 1558.35 nm, then the net cavity dispersion is estimated to be  $\sim 50 \text{ fs}^2$ . The SESAM has 18% modulation depth, 30% absorbance and 5 ps recovery time.

The 976 nm pump light is coupled into the gain fiber through a wavelength division multiplexer (WDM) and the coated fiber ferrule. The output pulses from the oscillator are injected into a three-stage EDF amplifier for amplification and compression. After each amplifier, an isolator is used to eliminate the influence of the unabsorbed pump light. The type of the EDFs in the three-stage amplifier is Liekki Er110-4/125. The optical spectrum of the pulses is measured by an optical spectrum analyzer (AQ6370D, Yokogawa). The radio frequency (RF) signal is detected by a high speed photodetector (UPD-15-IR2, Alphas) and the RF spectrum and phase noise is directly measured by a signal analyzer (FSUP26, Rohde & Schwarz).

### 3. Results and discussion

The oscillator realizes self-started mode-locking at a threshold pump power of 214 mW with a  $57 \mu\text{W}$  output power at a central wavelength of 1558.3 nm. At a threshold pump power of 214 mW, self-started mode locking state with a signal power of  $57 \mu\text{W}$  is achieved. While the pump power increases to 284 mW, the output power grows linearly to  $66 \mu\text{W}$ . The continuous wave (CW) mode-locked state turns to multi-pulsing state when the pump power is higher than 284 mW. Compared with the 27.4 mW output power in [24], the low output power in this work is due to the low output ratio (0.2%) and the high cavity loss caused by the mismatch between the EDF and single mode fiber (Corning SMF-28) in the output coupler, whose core diameters are 3 and  $8.5 \mu\text{m}$  respectively (provided by the manufacture).

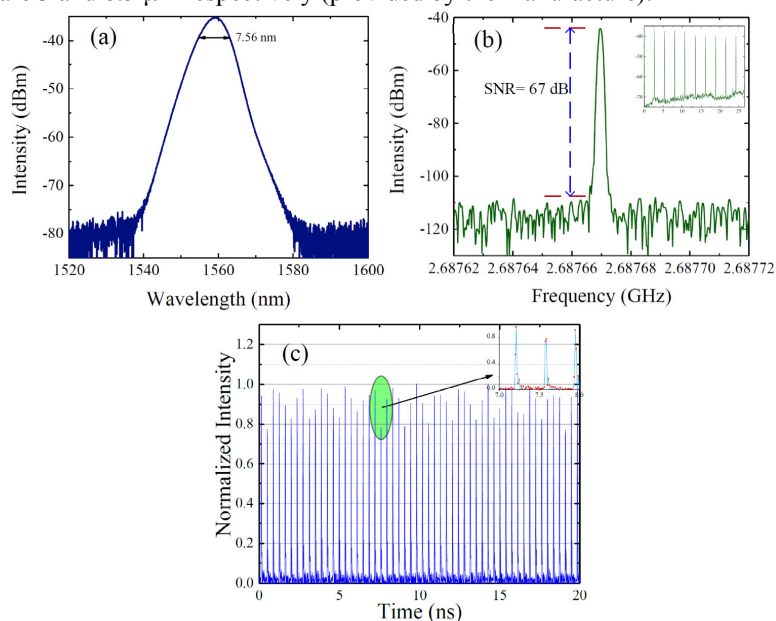


Fig. 2. (a) Optical spectrum from the oscillator. (b) RF spectrum of the oscillator with a resolution bandwidth of 1 kHz. Inset: wide-span RF spectrum. (c) Pulse train of the oscillator with 2.68 GHz pulse repetition rate.

Figure 2(a) illustrates the optical spectrum of the output pulses measured at 232 mW pump power. The optical spectrum has a central wavelength of 1558.35 nm and a 3 dB spectral bandwidth of 7.56 nm. As shown in Fig. 2(b), the RF spectrum indicates a 2.68 GHz

fundamental pulse repetition rate and a 67 dB signal-to-noise ratio (SNR). The resolution bandwidth and span are 1 kHz and 100 kHz, respectively. The inset to Fig. 2(b) shows the broad RF spectrum of the harmonics in a full span of 26.5 GHz. The pulse train of the oscillator is depicted in Fig. 2(c), the corresponding temporal period is 372.07 ps, indicating the fundamental cavity frequency of 2.68 GHz. The fluctuation of the peak values is caused by the insufficient sampling rate, the details of the sampled pulses can be seen in the inset where the red square dot is the sampling point. The mode-locked waveform of the oscilloscope trace and the clear intensity of the RF spectrum demonstrate that the oscillator is operating at CW mode-locked state.

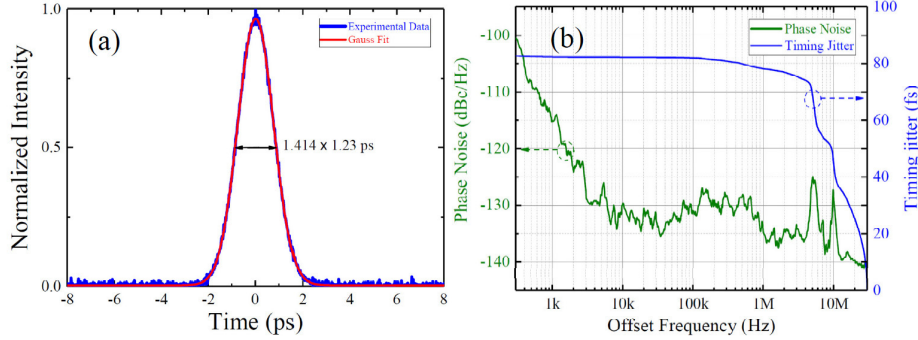


Fig. 3. (a) The measured intensity autocorrelation trace and Gaussian fit of the pre-amplified optical pulses. (b) The measured single sideband (SSB) phase noise and the integrated timing jitter.

In order to measure the intensity autocorrelation trace and phase noise, the output power of the oscillator is pre-amplified to 3 mW. The intensity autocorrelation trace (measured by HAC-200, Alnair Labs) displayed in Fig. 3(a) has a full width at half-maximum (FWHM) width of 1.74 ps, corresponding a temporal width of 1.23 ps when a Gaussian pulse shape is assumed.

The single sideband (SSB) phase noise measured at 2.68 GHz fundamental frequency is displayed in Fig. 3(b). The phase noise at 300 Hz offset is below -100 dBc/Hz and decreases to -130 dBc/Hz with the offset frequency increasing to 10 kHz. For the offset frequencies higher than 10 kHz, the phase noise fluctuates between -130 and -140 dBc/Hz. The timing jitter integrated from 30 MHz progressively down to 300 Hz is given as the blue line in Fig. 3(b), resulting in an integrated jitter of 82.5 fs over the entire frequency interval. In [24] the timing jitter integrated from 10 MHz down to 1 kHz is 22 fs, which is the best reported timing jitter among the fiber lasers with over 1 GHz repetition rate so far. Though our laser has a higher repetition rate and a broader integral interval (from 30 MHz down to 300 Hz) is selected, small timing jitter of 82.5 fs is obtained.

The theory models of noise properties of mode-locked lasers have been built in [28-32]. According to [32], the power spectral density (PSD) of timing jitter contributed by amplified spontaneous emission (ASE) noise can be expressed as

$$S_{\Delta t} = 0.53 \frac{\theta h \nu l_{tot}}{E_p T_{rt}} \tau_p^2 \frac{1}{(2\pi f)^2} + \left( \frac{D_2}{f T_{rt}} \right)^2 S_{vc}(f). \quad (1)$$

Here  $\theta$  is the spontaneous emission factor of the active fiber,  $\nu$  is the frequency of the optical pulse,  $E_p$  is the pulse energy,  $l_{tot}$  is the total intracavity losses per round trip,  $\tau_p$  is the pulse duration,  $T_{rt}$  is the round-trip time,  $f$  is the noise frequency,  $D_2$  is the group delay dispersion (GDD) and  $S_{vc}(f)$  represents the fluctuations of the “center of gravity” of the optical frequency spectrum (mean optical frequency):

$$S_{vc}(f) \approx 0.53 \frac{\theta h \nu l_{tot}}{E_p T_{rt}} \Delta \nu_p^2 \frac{1}{(2\pi f)^2 + \tau_{vc}^{-2}}, \quad (2)$$

where the filter time constant  $\tau_{vc}$  is given by

$$\tau_{vc} \approx 0.47 \frac{T_{rt}}{g} \left( \frac{\Delta \nu_g}{\Delta \nu_p} \right)^2, \quad (3)$$

here,  $\Delta \nu_g$  and  $\Delta \nu_p$  are gain bandwidth and pulse bandwidth respectively.

For noise frequencies below tens of kilohertz, the dominant noise source is classical noise which originates from pump noise and cavity length fluctuations. For noise frequencies above tens of kilohertz, the ASE noise mainly contributes to the timing jitter. There are two different way for ASE noise to influence the timing jitter: (i) the first term on right hand side of Eq. (1) describes the direct effect of ASE noise by causing a random shift of the pulse position; (ii) the second term shows the indirect effect of ASE noise. Explicitly, when GDD is present, the fluctuations of the mean optical frequency originating from the ASE noise can be translated into timing jitter, which is called Gordon-Haus jitter. For the oscillator in this work, the total net cavity dispersion is near zero ( $\sim 50 \text{ fs}^2$ ), so that the Gordon-Haus jitter is reduced dramatically, the contribution to the timing jitter are mainly due to the direct influence of ASE noise. According to Eq. (1), the small round-trip time  $T_{rt}$  and high spontaneous emission  $\theta$ , which are necessary for gigahertz fiber lasers, lead to higher timing jitter compared with  $\sim 100$  MHz fiber lasers. The jitter is also increased by high cavity loss  $l_{tot}$ , which originates from the non-saturable loss of SESAM and the different core diameters of the EDF and single mode fiber in the output coupler. Besides, both the low intracavity pulse energy  $E_p$  and long pulse duration  $\tau_p$  could lead to high timing jitter. It might be an effective way to optimize the timing jitter via reducing cavity loss by using an EDF with a core diameter of  $\sim 8.5 \mu\text{m}$ . Besides, we can choose SESAMs with lower non-saturable loss and smaller recovery time which could also reduce cavity loss and shorten pulse duration. The feedback control of pump power and fiber length is also helpful to reduce the influence of classical noise to timing jitter.

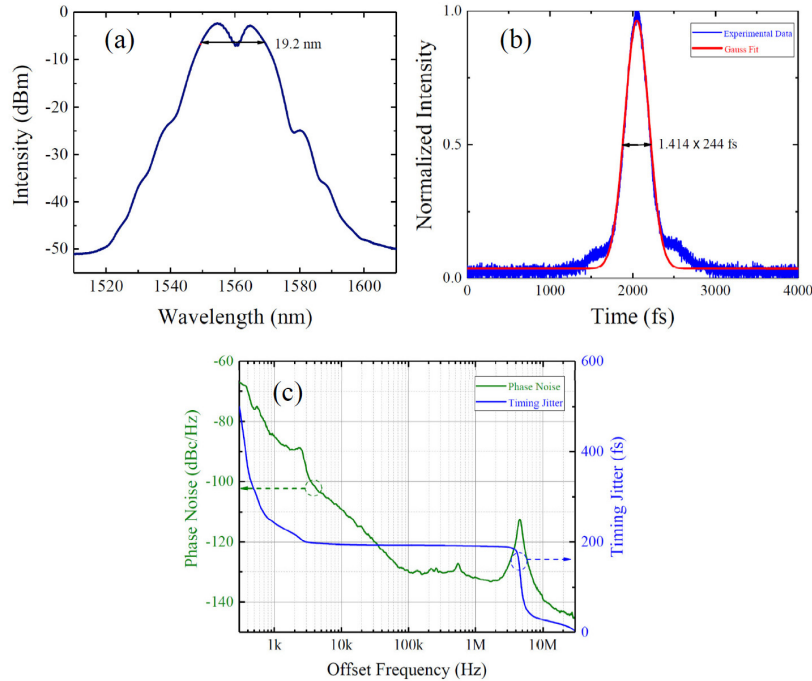


Fig. 4. (a) The broadened optical spectrum measured after a three-stage amplifier. (b) The corresponding intensity autocorrelation trace. (c) The phase noise and timing jitter of the amplified optical pulses.

The average power of the optical pulses from oscillator is amplified to 430 mW by the three-stage amplifier. Due to nonlinear self-phase modulation effect and the symmetrical shape of the input pulses, the 3 dB bandwidth of the optical spectrum is symmetrically broadened to 19.2 nm, as shown in Fig. 4(a). Then the amplified optical pulses propagate through a 1.5 m single mode fiber (Corning SMF-28) for compression. Fig. 4(b) shows the measured intensity autocorrelation trace of the compressed pulses (measured by FR103MN autocorrelator, Femtochrome Research INC.), which gives a temporal pulse width of 244 fs if a Gaussian pulse shape is assumed, and the Gaussian fitting curve matches well with the experimental data. The pulse width is slightly longer than the 183 fs transform-limited duration, which indicates that the pulses are chirped. The phase noise and timing jitter of the amplified pulses are presented in Fig. 4(c). Compared with the results in Fig. 3(b), the phase noise is deteriorated and the timing jitter increases from 82.5 fs to 496.2 fs. The peak at around 5 MHz on the phase noise curve is caused by the excess ASE noise in the third-stage amplifier. The results demonstrate that the ASE noise from the amplifiers greatly affects the noise properties of the optical pulses. Further optimization of the three-stage amplifier is needed to obtain a better noise performance of the laser.

#### 4. Conclusion

We demonstrate a 2.68 GHz fundamental repetition rate Er-doped passively mode-locked all fiber laser and investigate the amplification and compression of the high repetition rate pulses. The compact and robust oscillator operates at a central wavelength of 1558.35 nm and spectral bandwidth of 7.56 nm. The SNR of the RF spectrum is 67 dB and the timing jitter integrated from 30 MHz to 300 Hz is 82.5 fs, which exhibits low timing jitter performance of the high repetition rate passively mode-locked fiber laser. A detailed characterization of the timing jitter is present. To eliminate the Gordon-Haus jitter, the oscillator is designed to operate at the regime where the net cavity dispersion is near zero. Meanwhile, the approaches to further optimize the timing jitter are also proposed. After a three-stage amplification and compression, an average power of 430 mW, a broadened spectral bandwidth of 19.2 nm and a compressed pulse duration of 244 fs are achieved. The laser we present promises a valuable optical source for many practical applications such as astro-combs, low-noise microwave generation and so on.

#### Funding

This work was supported by National key R&D Program of China (2016YFF0200700) and Natural Science Foundation of China (61875226).

#### References

1. S. T. Cundiff, and A. M. Weiner, "Optical arbitrary waveform generation," *Nat. Photonics* **4**(11), 760-766 (2010).
2. A. Rashidinejad, D. E. Leaird, and A. M. Weiner, "Ultrabroadband radio-frequency arbitrary waveform generation with high-speed phase and amplitude modulation capability," *Opt. Express* **23**(9), 12265-12273 (2017).
3. D. J. Jones, S. A. Diddams, J. K. Ranka, A. Stentz, R. S. Windeler, J. L. Hall, and S. T. Cundiff, "Carrier envelope phase control of femtosecond mode-locked lasers and direct optical frequency synthesis," *Science* **288**(5466), 635-640 (2000).
4. T. M. Fortier, A. Bartels, and S. A. Diddams, "Octave-spanning Ti:sapphire laser with a repetition rate > 1 GHz for optical frequency measurements and comparisons," *Opt. Lett.* **31**(7), 1011-1013(2013).
5. T. M. Fortier, M. S. Kirchner, F. Quinlan, J. Taylor, J. C. Bergquist, T. Rosenband, N. Lemke, A. Ludlow, Y. Jiang, C. W. Oates, and S. A. Diddams, "Generation of ultrastable microwaves via optical frequency division," *Nat. Photonics* **5**(7), 425-429 (2011).
6. T. M. Fortier, A. Rolland, F. Quinlan, F. N. Baynes, A. J. Metcalf, A. Hati, A. D. Ludlow, N. Hinkley, M. Shimizu, T. Ishibashi, J. C. Campbell, and S. A. Diddams, "Optically referenced broadband electronic synthesizer with 15 digits of resolution," *Laser Photonics Rev.* **10**(5), 780-790 (2016).
7. H. Jiang, J. Taylor, F. Quinlan, T. Fortier, and S. A. Diddams, "Noise floor reduction of an Er: fiber laser-based photonic microwave generator," *IEEE Photon. J.* **3**(6), 1004-1012 (2011).
8. J. Kim, M. J. Park, M. H. Perrott, F. X. Kärtner, "Photonic subsampling analog-to-digital conversion of

- microwave signals at 40-GHz with higher than 7-ENOB resolution,” *Opt. Express* **16**(21), 16509-16515 (2008).
9. V. Vercesi, D. Onori, J. Davies, A. Seeds, and C. P. Liu, “Electronically synthesized Nyquist pulses for photonic sampling of microwave signals,” *Opt. Express* **25**(23), 29249-29259 (2017).
  10. H. Meng, J. Leng, C. Qian, and J. Zhao, “Optical sampling analog-to-digital converter based on two asynchronous mode-locked fiber lasers,” *J. Opt. Soc. Am. B* **34**(4), 824-830 (2017).
  11. R. A. McCracken, J. M. Charsley, and D. T. Reid, “A decade of astrocombs: recent advances in frequency combs for astronomy,” *Opt. Express* **25**(13), 15058–15078 (2017).
  12. M. Lezius, T. Wilken, C. Deutsch, M. Giunta, O. Mandel, A. Thaller, V. Schkolnik, M. Schiemangk, A. Dinkelaker, A. Kohfeldt, A. Wicht, M. Krutzik, A. Peters, O. Hellmig, H. Duncker, K. Sengstock, P. Windpassinger, K. Lampmann, T. Hülasing, T. W. Hänsch, and R. Holzwarth, “Space-borne frequency comb metrology,” *Optica* **3**(12), 1381–1387 (2016).
  13. V. Torres-Company, and A. M. Weiner, “Optical frequency comb technology for ultra-broadband radio-frequency photonics,” *Laser Photonics Rev.* **8**(3), 368–393 (2014).
  14. P. Zou, T. Steinmetz, A. Falkenburgher, Y. Wu, L. Fu, M. Mei, R. Holzwarth, “Broadband Frequency Comb for Calibration of Astronomical Spectrographs,” *Journal of Applied Mathematics and Physics* **04**, 202-205 (2016).
  15. H.-W. Chen, G. Chang, S. Xu, Z. Yang, and F. X. Kärtner, “3 GHz, fundamentally mode-locked, femtosecond Yb-fiber laser,” *Opt. Lett.* **37**(17), 3522–3524 (2012).
  16. H. Cheng, W. Wang, Y. Zhou, T. Qiao, W. Lin, S. Xu, and Z. Yang, “5 GHz fundamental repetition rate, wavelength tunable, all-fiber passively mode-locked Yb-fiber laser,” *Opt. Express* **25**(22), 27646-27651 (2017).
  17. C. Li, G. Wang, T. Jiang, A. Wang, Z. Zhang, A. M. Wang, and Z. G. Zhang, “750 MHz fundamental repetition rate femtosecond Yb: fiber ring laser,” *Opt. Lett.* **38**(3), 314–316 (2013).
  18. B. Xu, H. Yasui, Y. Nakajima, Y. Ma, Z. G. Zhang, and K. Minoshima, “Fully stabilized 750-MHz Yb: fiber frequency comb,” *Opt. Express* **25**(10), 11910-11918 (2017).
  19. H. Cheng, W. Lin, Z. Luo, and Z. Yang, “Passively mode-locked Tm<sup>3+</sup>-doped fiber laser with gigahertz fundamental repetition rate,” *IEEE J. Sel. Top. Quantum Electron.* **24**(3), 1100106 (2018).
  20. H. Cheng, W. Lin, T. Qiao, S. Xu, and Z. Yang, “Theoretical and experimental analysis of instability of continuous wave mode locking: Towards high fundamental repetition rate in Tm<sup>3+</sup>-doped fiber lasers,” *Opt. Express* **24**(26), 29882–29895 (2016).
  21. A. Martinez and S. Yamashita, “Multi-gigahertz repetition rate passively modelocked fiber lasers using carbon nanotubes,” *Opt. Express* **19**(7), 6155-6163 (2011).
  22. A. Martinez and S. Yamashita, “10 GHz fundamental mode fiber laser using a graphene saturable absorber,” *Appl. Phys. Lett.* **101**(4), 041118 (2012).
  23. S. Y. Set, S. Yamashita, K. Hsu, K. H. Fong, Y. Inoue, K. Sato, D. Tanaka, and M. Jablonski, “5 GHz pulsed fiber Fabry-Pérot laser mode-locked using carbon nanotubes,” *IEEE Photonics Technol. Lett.* **17**(4), 750–752 (2005). C. Li, G. Wang, T. Jiang, A. Wang, Z. Zhang, A. M. Wang, and Z. G. Zhang, “750 MHz fundamental repetition rate femtosecond Yb: fiber ring laser,” *Opt. Lett.* **38**(3), 314–316 (2013).
  24. H. Byun, M. Y. Sander, A. Motamedi, H. Shen, G. S. Petrich, L. A. Kolodziejski, E. P. Ippen, and F. X. Kärtner, “Compact, stable 1 GHz femtosecond Er-doped fiber lasers,” *Appl. Opt.* **49**(29), 5577–5582 (2010).
  25. H. Byun, D. Pudo, J. Chen, E. P. Ippen, and F. X. Kärtner, “High-repetition-rate, 491 MHz, femtosecond fiber laser with low timing jitter,” *Opt. Lett.* **33**(19), 2221-2223 (2008).
  26. R. Thapa, D. Nguyen, J. Zong, and A. Chavez-Pirson, “All-fiber fundamentally mode-locked 12 GHz laser oscillator based on an Er/Yb-doped phosphate glass fiber,” *Opt. Lett.* **39**(6), 1418–1421 (2014).
  27. J. J. McFerran, L. Nenadović, W. C. Swann, J. B. Schlager, and N. R. Newbury, “A passively mode-locked fiber laser at 1.54  $\mu\text{m}$  with a fundamental repetition frequency reaching 2GHz,” *Opt. Express* **15**(20), 13155-13166 (2007).
  28. D. von der Linde, “Characterization of the noise in continuously operating mode-locked lasers,” *Appl. Phys. B* **39**(4), 201–217 (1986).
  29. H. A. Haus, and A. Mecozzi, “Noise of mode-locked lasers,” *IEEE J. Quantum Electron.* **29**(3), 983 (1993).
  30. R. Paschotta, “Noise of mode-locked lasers (Part I): numerical model,” *Appl. Phys. B* **79**(2), 153-162 (2004).
  31. R. Paschotta, “Noise of mode-locked lasers (Part II): timing jitter and other fluctuations,” *Appl. Phys. B* **79**(2), 163-173 (2004).
  32. R. Paschotta, “Timing jitter and phase noise of mode-locked fiber lasers,” *Opt. Express* **18**(5) 5041-5054 (2010).
  33. Y. Song, C. Kim, K. Jung, H. Kim, and J. Kim, “Timing jitter optimization of mode-locked Yb-fiber lasers toward the attosecond regime,” *Opt. Express* **19**(15), 14518-14525 (2011).